CONF-8907168--1

UCRL--100359

DE90 002978

INTENSE REB TRANSPORT IN A WEAKLY MAGNETIZED PLASMA

J. F. Camacho
B. R. Poole
B. Chang

This paper was prepared for submittal to

IEEE Seventh Pulsed Power Conference
Monterey, CA.

June 11-14, 1989

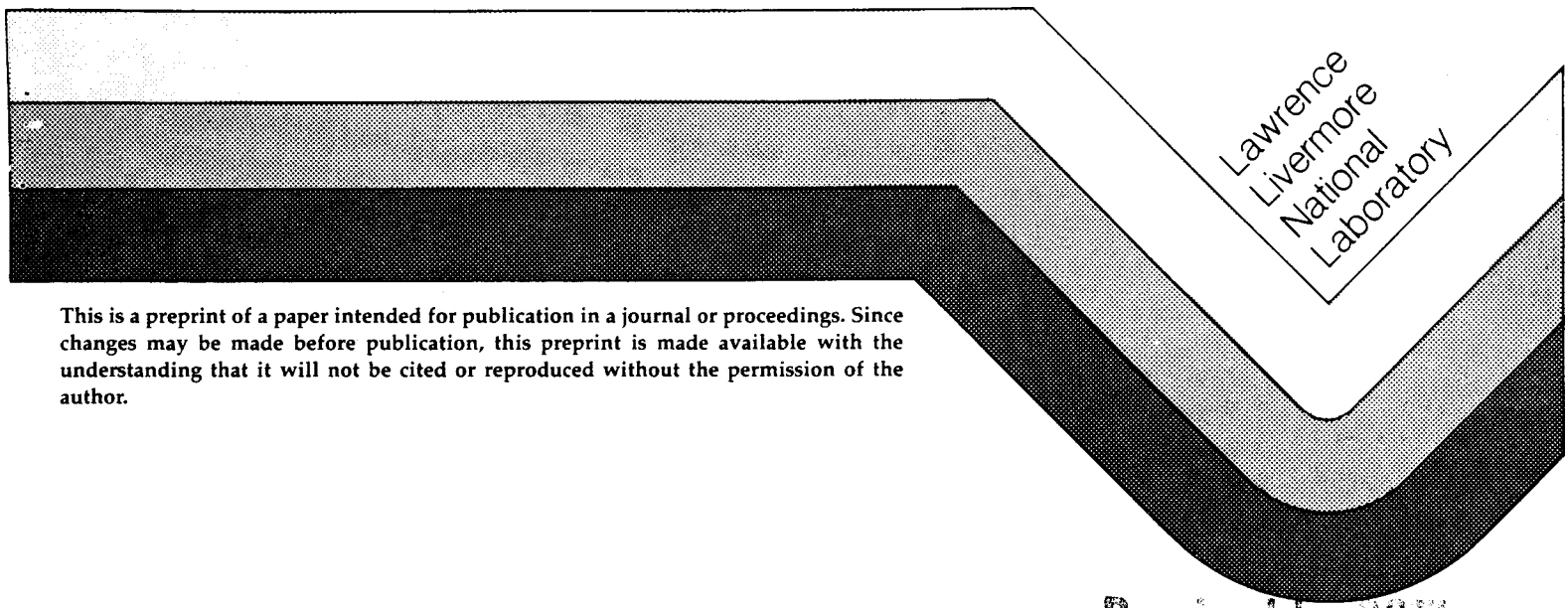

INTENSE REB TRANSPORT IN A WEAKLY MAGNETIZED PLASMA*

J. F. CAMACHO, B. R. POOLE, B. CHANG

Lawrence Livermore National Laboratory
University of California
Livermore, CA 94550

Abstract

Intense relativistic electron beams (REBs) have been used in various applications for the purpose of high-power microwave (HPM) generation. By injecting the beam into a plasma, it is possible to overcome the space-charge limiting current because of charge and current neutralization provided by the plasma. Our goal in this experiment was to study beam transport issues which may be relevant to the development of HPM sources which use intense REBs.

We conducted high-power REB-plasma interaction experiments by injecting a 1.4 MeV, 25 kA electron beam with $n_b \approx 4 \times 10^{10}\,\mathrm{cm}^{-3}$ into a preformed, partially ionized (< 1 %) argon background situated within a 15 cm ID Lucite tube, with $n_e \sim 10^{11}\,\mathrm{cm}^{-3}$. Our experimental apparatus consisted of the electron beam accelerator, a plasma source, magnetic field coils, and beam, plasma, and microwave diagnostics. The beam diagnostics included a streak camera and Rogowski coils to measure beam profiles and net current in the system, respectively. A microwave interferometer provided plasma density measurements around the time of the beam-plasma interaction. We also measured RF emission using a microwave spectrometer. These data will be presented.

Particle-in-cell code simulations have been performed to help us understand the relevant physics. We shall present the results of these computations.

Introduction

Much work has been done to study the interaction of a relativistic electron beam with a background plasma. Our research at LLNL was prompted by the experimental results of investigators at UC Irvine, who reported observing intense microwave emission over a broad band of frequencies (1 to 100 GHz) when the density of electrons in the beam closely matched the density of electrons in the plasma [1,2].

According to theory, the microwave generation mechanism consists of setting up a two-stream instability in which the beam interacts with the return current which the beam has induced in the plasma. This instability gives rise to electrostatic potentials in the plasma which in turn modulate the beam current so as to cause microwave emission. We have experimented with beam-plasma parameters similar to those of the Irvine apparatus. A 1.4 MeV, 35 kA electron beam was injected into an unmagnetized plasma situated in a 1 m long Lucite tube in which $n_e \sim 10^{11}\,\mathrm{cm}^{-3}$. We have reported the results of that work [3]. Based upon our microwave emission measurements and our theoretical and computational work, we concluded that two fundamental changes had to be made in our experiment in order for it to become a reasonably efficient source of high-power microwaves (HPM). First, an axial magnetic field had to be added to ensure laminar beam transport. (The high beam current made it very likely that our beam was pinching off and thus not interacting fully with the plasma background.) Second, a metallic waveguide rather than a dielectric vessel should be used to contain the plasma. Such a structure would allow coupling of the electrostatic oscillations of the two-stream instability to the electromagnetic fields of the waveguide, giving rise to coherent microwave radiation. The addition of these two features alters in a fundamental way the physical mechanism by which the microwaves are generated. This type of microwave source would thus be qualitatively different from the one discussed in [3].

Experimentally, therefore, our objective was to begin making the transition to this new type of device. The first step was to examine beam propagation and microwave generation by conducting experiments in which an axial magnetic field of about 1.7 kG was applied. On the theoretical and computational side, we have carried out a modeling effort in order to increase our understanding of the beam propagation and microwave generation issues.

Experimental Work

Considerable effort went into modifying our apparatus in order to accommodate the addition of the four 16 inch diameter coils used to produce the axial magnetic field. Figure 1 shows the arrangement of the system. We proceeded to conduct a shot series on our accelerator to study beam transport and measure microwave emission. Our diagnostics consisted of a streak camera and Rogowski coils used for beam transport studies, and a microwave spectrometer used to record the RF emission. We also set up our microwave interferometer diagnostic to measure plasma density during the interaction, as we have done previously [4]. In our beam-plasma experiments, our standard shot was to fire the beam into an argon plasma with $n_e \sim 10^{11}\,\mathrm{cm}^{-3}$. The neutral background fill consisted of 2 mT of argon gas.

The presence of an axial magnetic field modified the operation of our plasma source. Unlike the zero magnetic field case, in which the plasma filled up the volume of the Lucite tube more or less uniformly, the plasma was now constricted predominantly to a column whose radius was that of the LaB_6 disk and electrode used to produce it (about 2.5 cm; see Fig. 1). We found that for a given current used to ionize the argon gas, much higher plasmas densities could be attained and with much longer decay times, as would be expected due to the presence of the magnetic field (see Fig. 2). The firing of beam, which propagates on a much faster time scale than that of the plasma decay, is timed so that it is injected into the system during the afterglow at the point in time corresponding to a plasma electron density of about $10^{11}\,\mathrm{cm}^{-3}$.

The reduced size of the plasma meant that the radius of our beam could be no larger that 2.5 cm, because in order to achieve current neutralization and ensure adequate beam transport, the entire beam has to propagate within the plasma. The field emission diode being used, however, had a radius of about 6 cm, thus necessitating some form of aperturing in order to reduce the beam size. This implied a reduction in the beam

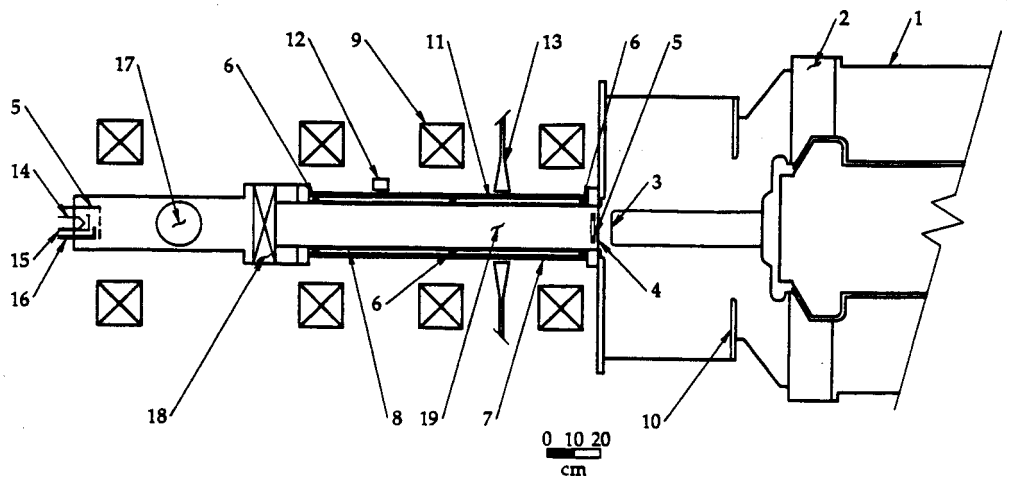

1. Water dielectric
2. Insulator
3. Cathode
4. Anode foil
5. Plasma source anode
6. Rogowski coils
7. Current return rods
8. Lucite tube
9. B-field coils
10. Vacuum current monitors
11. Microwave absorbing foam
12. 2–18 GHz antenna
13. Interferometer horns
14. Heater filament
15. Lanthanum hexaboride cathode
16. Argon fill tube
17. Vacuum pump port
18. Gate valve
19. Argon gas/plasma fill

Figure 1—Experimental apparatus.

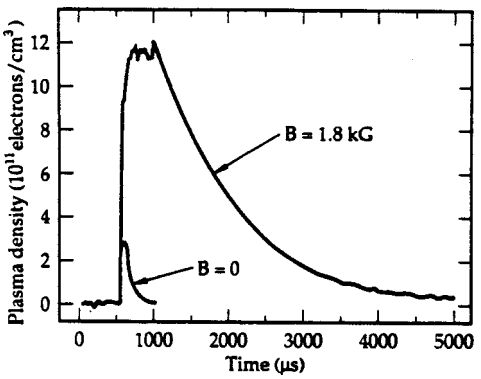

Figure 2—Plot of plasma density *vs.* time with and without axial magnetic field (no beam fired) with a background fill of 2 mT of argon. The axial field enables us to produce plasmas with higher densities and longer decay times. For an actual accelerator shot, the beam is fired at a predetermined time corresponding to the desired density. In our case, that is usually around $n_e = 10^{11}$ cm^{-3}.

current which we would propagate, but the beam would still be sufficiently intense to provide us with a suitable measurement of beam transport in the regime of interest.

Before firing into plasma, however, we first injected the beam into a 4 cm vacuum drift space and measured the beam profile using a streak camera. We performed these measurements both with the magnetic field on and off in order to compare the difference, and the results are shown in Figs. 3 and 4. For the sake of obtaining some idea of what the radius or width of the beam is in each case, a gaussian profile was fitted to each set of data points. We found that with the magnetic field on, the beam appears to be more concentrated and collimated, as indicated by the smaller radius (2.3 cm *vs.* 3.7 cm) and the fact that the intensity of the beam was stronger. This higher intensity indicates that the beam current injected into the drift region was larger when the magnetic field was on. (No direct measurement of the beam current actually flowing in the drift space was available when we used this diagnostic; only the accelerator current was measured.) With the magnetic field off, it appears that the beam current is "sprayed" off the cathode in a more diffuse fashion. Hence, less current actually makes it past the anode, into the drift region, and through the pinholes which create the beamlets that are observed by the streak camera. These results lead us to believe that we obtain better beam propagation when the axial magnetic field is on, as expected.

We then proceeded to conduct experiments in which the beam was injected into the argon plasma. Three Rogowski coils located at entrance, middle, and end of the Lucite tube measured net current in the system, and our microwave interferometer was used to record the plasma density before, during, and after shot time. A 2-18 GHz flat frequency response cavity-backed spiral antenna fed the RF signal from the emitted microwaves into our pulse spectrometer, which sorts it into several frequency subbands.

Data from one of our beam-plasma shots are shown in Figs. 5–7. As was the case with all such shots, some fraction of the accelerator current does not make its way into the interaction region, presumably due to losses incurred by electrons which are "sprayed" off the diode at an angle and hit the front plate of the accelerator. Furthermore, we expect to see current neutralization take place almost immediately at the head of the beam, and this too may explain why the net current is less than the accelerator current from the outset. A return current is established in the plasma, reducing the net current in the system, which is what can be measured. About 40% of the net current at the injection point appears at the end of the interaction region, 1 m away. We suspect that all the beam current does in fact propagate to the end of the tube, but a considerable fraction of it is neutralized by the plasma return current. We surmise that beam propagation in an axial magnetic field was adequate, but our simulations indicate that a higher value of the field (around 4 kG or more) is desirable in order to ensure high-quality beam transport (*i.e.*, reduced

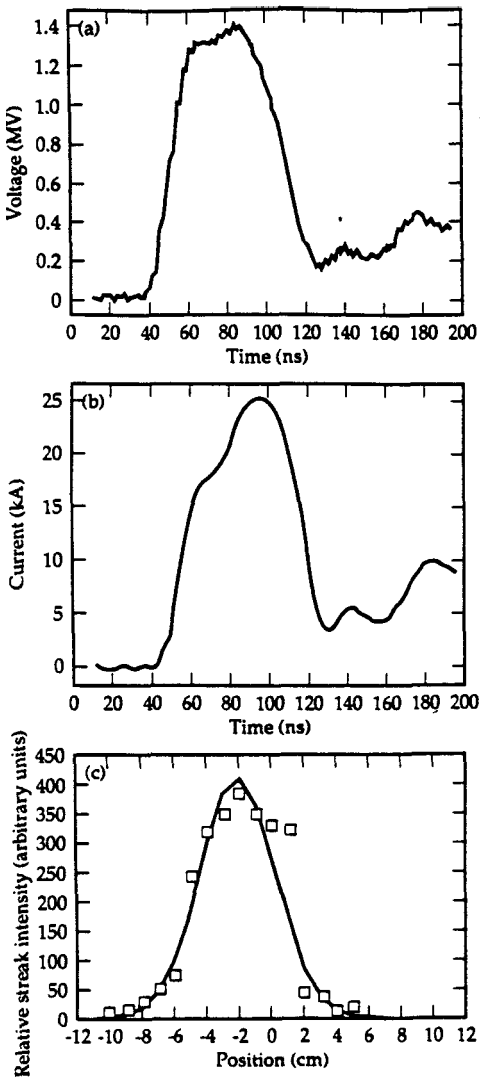

Figure 3—Streak camera measurements of beam profile in the presence of the magnetic field. (a) Accelerator voltage *vs.* time. (b) Accelerator current *vs.* time. (c) Radial profile of beam taken at peak of beam pulse.

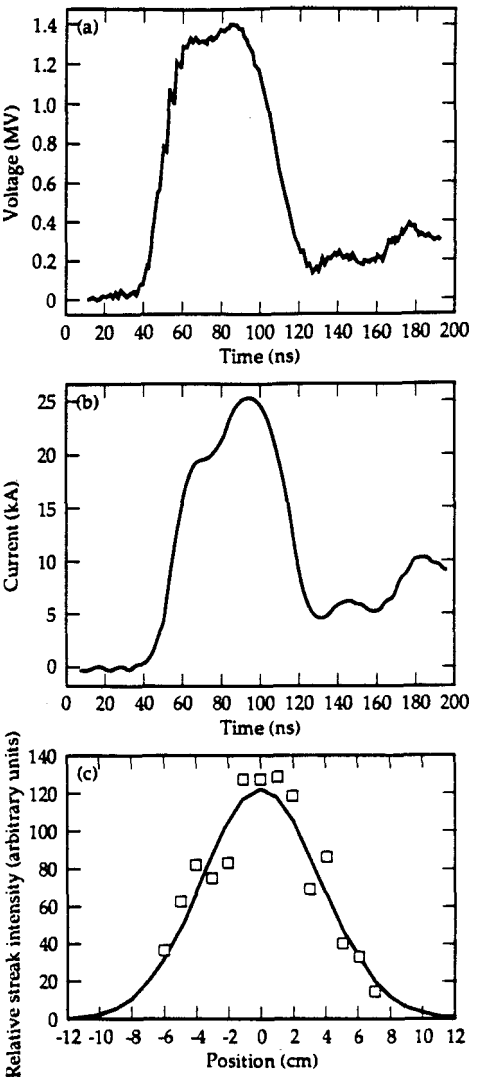

Figure 4—Streak camera measurements of beam profile in the absence of the magnetic field. (a) Accelerator voltage *vs.* time. (b) Accelerator current *vs.* time. (c) Radial profile of beam taken at peak of beam pulse.

transverse motion of the beam).

As we have done previously, we also performed measurements of the plasma density during an actual shot using our microwave interferometer diagnostic operating at 30.9 GHz. Figure 6 is a plot of the density around shot time. It shows that the electron density increases slightly immediately after the beam has passed through the plasma, and then it begins to increase substantially later in time, eventually reaching densities of at least $n_e \sim 10^{13}\,\mathrm{cm}^{-3}$ several microseconds after the shot. These results are consistent with what we observed during our shot series last year [4]. The increase in density occurring after the beam pulse interacts with the plasma is greater than one would expect simply from beam-induced impact ionization, but other mechanisms (such as beam-induced plasma heating) may accelerate plasma electrons so as to bring about the observed ionization. We are confident that the plasma density does not change significantly during the actual beam-plasma interaction. (The apparent density increase seen in Fig. 6 during the beam pulse is artificial, as it arises from microwave "pollution" brought about by the emission which takes place at the time.) This is an important result, as the ratio of beam density to plasma density is a key parameter in this experiment and is something which we need to be able to control fairly well.

As far as microwave generation was concerned, the presence of the axial magnetic field did not yield any dramatic or even noticeable improvements over past performance without the field [3]. In Fig. 7, we show a typical plot of microwave emission in the 6-7 GHz band. Unfortunately, we were not able to obtain good measurements in the 2-6 GHz band, which is of more interest to us. However, the indications which we have available lead us to conclude that, without a waveguide in which the beam-plasma interaction can take place, this device is a low-power and very inefficient microwave generator.

Calculational Work

The calculational work seeks to address two issues: first, the nature of the transport of a relativistic electron beam in a plasma, and second, to understand the various instabilities associated with this physical system, some of which may be exploited for the production of high-power microwaves. Both of these issues are intimately related and require a balance of both analytic computations and particle-in-cell (PIC) code simulations to understand the complex physical phenomena associated with this problem.

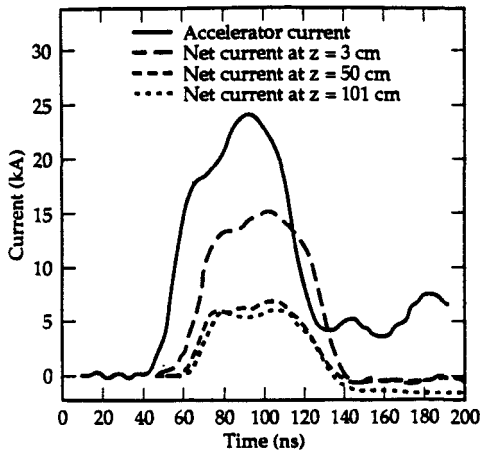

Figure 5—Beam-plasma shot data. (a) Accelerator current *vs.* time. (b) Net current at $z = 3\,\text{cm}$ *vs.* time. (c) Net current at $z = 50\,\text{cm}$ *vs.* time. (d) Net current at $z = 101\,\text{cm}$ *vs.* time.

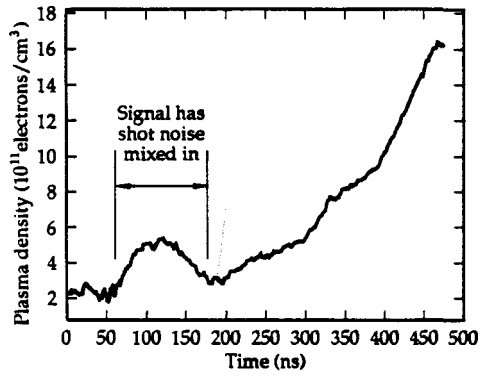

Figure 6—Plasma density *vs.* time during a shot. The apparent increase in density around 125 ns is due to noise from the microwave emission occurring as the beam and plasma interact.

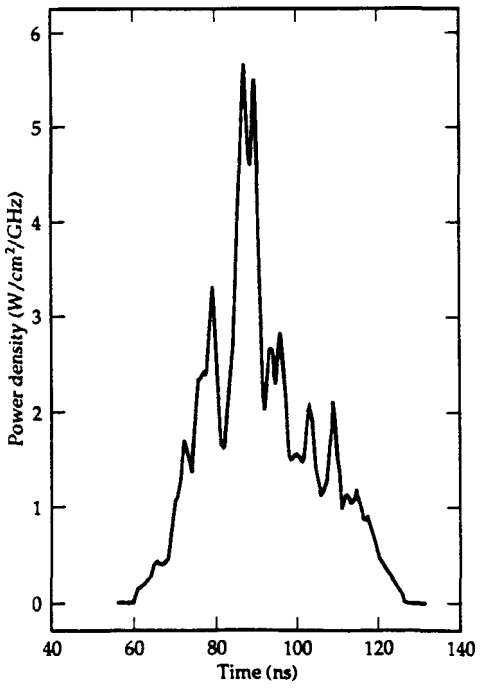

Figure 7—Microwave emission in the 6-7 GHz band *vs.* time.

In contrast to low-current electron beams, a system utilizing an intense beam can modify the zero-order solutions of the coupled particle-field equations in the sense that the solutions are no longer homogeneous or stationary. The nature of the zero-order solutions are crucial for the development of the dispersion relation of the system which is required to understand the instabilities of the system.

The strength of the external axial magnetic field is an important parameter for both issues of this problem. In the infinite magnetic field limit, the particle motion becomes one-dimensional along the axial magnetic field and only the transverse magnetic (TM) modes of the plasma-filled waveguide are important for the analysis of the problem. However, in the finite magnetic field regime the particles of the plasma as well as of the electron beam can have transverse motion affecting both the zero-order and higher order solutions of the problem. This allows the transverse electric (TE) modes to become coupled to the TM modes due to the cyclotron motion of the electrons. Hence, in the finite magnetic field case both the two-stream and cyclotron instabilities are important.

We have extensively investigated the large magnetic field regime ($\omega_{ce} \gg \omega_{pe}, \omega_{be}$), both analytically and computationally. The full electromagnetic dispersion relation has been developed for this problem and a computer program was developed to determine the complex roots of this dispersion relation for both convective (amplifying) and absolute (oscillator) instabilities. The imaginary part of the complex root is the growth rate of the instability and the real part of the complex root gives the operating wavelength or temporal frequency of the system. The zero-order parameters (*e.g.*, plasma return current, beam velocity, *etc.*) are determined self-consistently from the self-generated fields associated with the beam front using analytic and PIC code results. These solutions are then used as parameters in the dispersion relation. A typical plot of the dispersion relation appears in Figs. 8a and 8b. Figure 8a shows the real part of the dispersion relation, demonstrating the coupling between the slow beam space-charge wave and the lower branch of the TM_{01} mode of the plasma filled waveguide. Figure 8b is a plot of the growth rate of the instability. We are presently developing the full electromagnetic dispersion relation for a bounded plasma in a finite axial magnetic field and are developing a computer program to determine the instabilities in this case. Again, the zero-order parameters are determined self-consistently and are used in the dispersion relation. The allowance of transverse motion of the beam and plasma adds many new branches to the dispersion relation and significantly complicates the calculation of the possible instabilities.

The problem has been studied utilizing CONDOR, a relativistic, fully electromagnetic PIC code. CONDOR code calculations include determination of space charge and current neutralization of the beam as well as the development of any instabilities. In addition, temporal histories and Fourier transforms are calculated utilizing the time history post-processor. Simulations were performed for a variety of parameters including realistic laboratory parameters. For the typical laboratory parameters, we were primarily interested in determining the nature of the beam transport. Figures 9a and 9b show the nature of the beam transport through a plasma in the presence of a 1.7 kG axial magnetic field. Figure 9a shows the presence of beam "sausaging" and Fig. 9b shows the axial beam velocity *vs.* z. This simulation indicates that the 1.7 kG magnetic field is adequate for complete beam transport through the system but that the beam is not sufficiently laminar for efficient

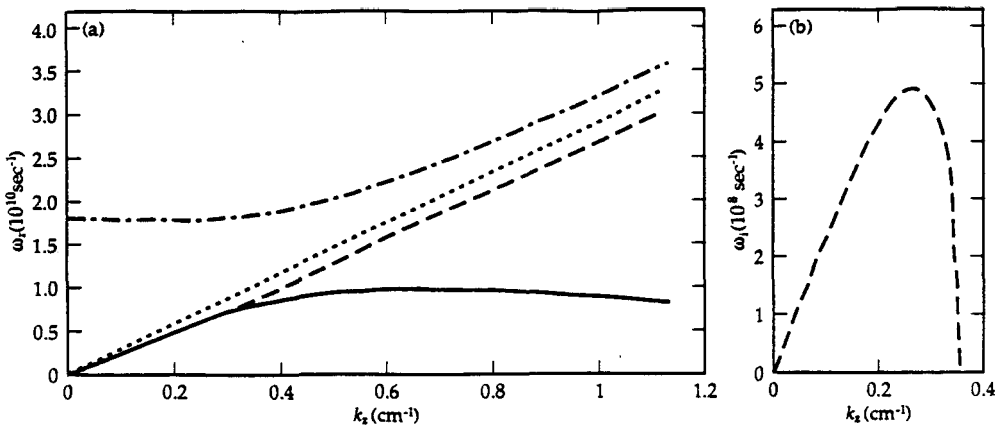

Figure 8—(a) The real part and (b) imaginary parts of $\omega(k_z)$ for a beam-plasma system. The real part gives the operating wavelength or temporal frequency of the system, while the imaginary part gives the growth rate of the instability. For both cases, the beam density is $2 \times 10^{11}\,\text{cm}^{-3}$ and the beam velocity is 0.941c. The plasma has a density of $8 \times 10^{11}\,\text{cm}^{-3}$ and a velocity of $-0.2c$.

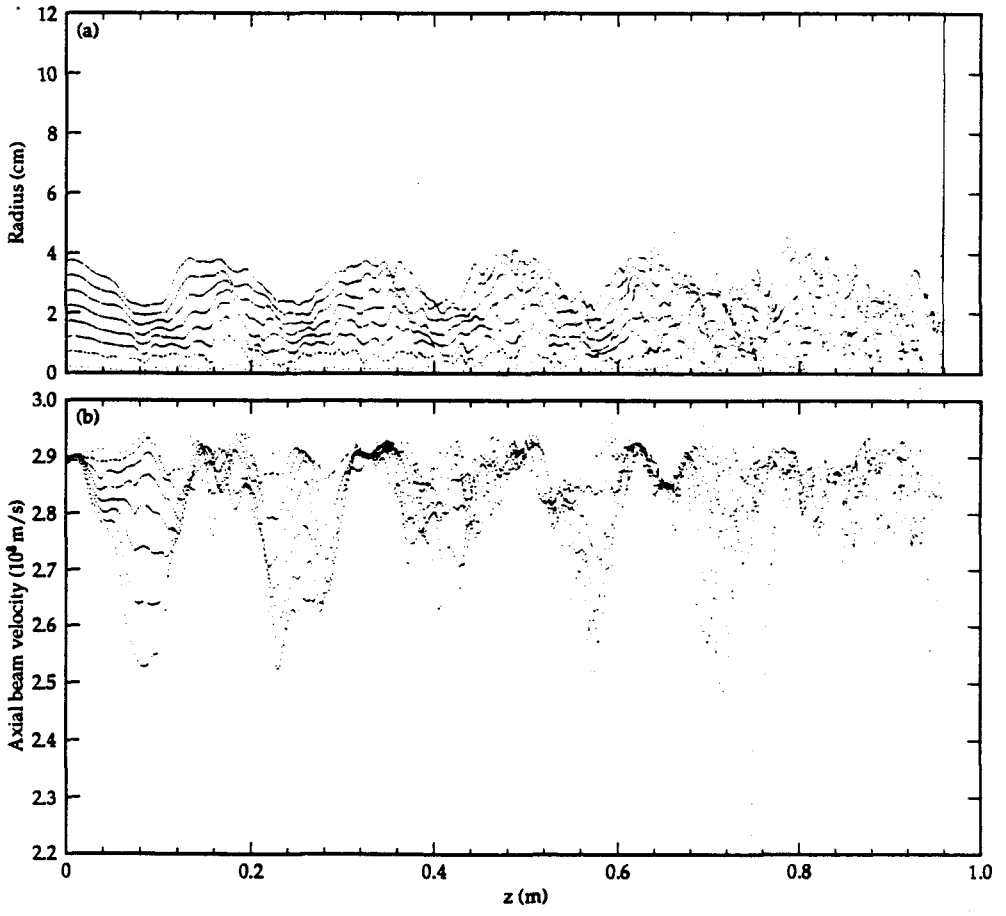

Figure 9—CONDOR simulation of beam transport through a plasma in the presence of a 1.7 kG axial magnetic field. (a) Propagation of a 1.4 MeV, 10 kA beam showing "sausaging" phenomenon. (b) Axial phase space of a 10 kA beam showing decrease in axial velocity as beam pinches inward. The beam values chosen represent typical laboratory parameters and hlep us determine the nature of the beam transport.

microwave production. These results compared favorably with the results from the laboratory experiments.

To gain additional insight into the relevant physics, a simulation was performed in the regime of very large magnetic fields. While these fields are not realistic for laboratory experiments, they do provide a basis from which to understand some of the important physical processes in this system. These results compared favorably with the analytic calculations for the infinite magnetic field regime but also demonstrated the presence of an instability not predicted by the linear theory. The simulation predicted additional higher frequencies from this device that were not predicted by the linear dispersion relation, and in fact this nonlinear instability could also produce coherent microwave radiation. Detailed study of the simulation results showed that a dense beam produces a potential well ahead of the beam due to the accumulation of plasma electrons in the process of space-charge neutralization. This propagating potential well moves at a velocity less than the injected beam velocity as well as less than the velocity of the unstable wave predicted by the linear theory. This accumulation of space charge eventually forms a potential well deep enough to backscatter the unstable wave which then mixes with the forward wave parametrically, upconverting ω and k_z to produce an electromagnetic wave on the upper branch of the TM_{01} dispersion curve. This upper branch electromagnetic wave operating slightly above the waveguide cutoff frequency can now forward scatter off the original unstable wave to provide still higher frequencies. Figure 10 is a representation of these mixing processes. Figures 11a and 11b show typical CONDOR results for the system utilizing a very large magnetic field. Figure 11a is a plot of the axial energy of the beam *vs.* z showing the slowing down of beam electrons in the beam front. Figure 11b shows the axial plasma electron velocity. The accumulation of space charge at the beam front and the current neutralized region behind the beam front can be seen. The large amplitude, long wavelength oscillations between $z = 0$ and $z = 1$ m correspond to the up-converted wave on the upper branch of the dispersion curves. Figures 12a and 12b show a typical temporal field history and its FFT, indicating the frequencies that are present in the wave mixing process (see Fig. 10).

Summary

Our experimental results indicate that beam transport in the 1.7 kG axial magnetic field was sufficiently good to assume successful propagation in any future experiments of this type. However, we do need to study in more depth the issue of current neutralization and its impact on beam transport. The PIC code simulations demonstrate that charge and current neutralization reduce the magnitude of the axial magnetic field required for laminar beam transport. In terms of microwave emission, there was no observable power increase due to the presence of the magnetic field. We conclude that in addition to having an axial magnetic field, the interaction must take place inside a metallic waveguide (as opposed to a dielectric vessel) in order for significant and efficient microwave gneration to occur in a beam-plasma device. This is supported by the results of our theoretical work and PIC code simulations. In addition, the simulations reveal the presence of radiation at higher frequencies than those predicted by linear theory. We postulate that this occurs by means of a three-wave parametric process.

Acknowledgements

* This work was performed by LLNL under U. S. Department of Energy contract no. W-7405-ENG-48. The authors gratefully acknowledge the assistance rendered by R. Druce and K. Griffin in setting up the streak camera apparatus and the help of R. Richardson in processing the streak camera data.

References

[1] K. Kato, G. Benford, and D. Tzach, "Detailed spectra of high-power broadband microwave emission from intense electron-beam plasma interactions," *Phys. Rev. Lett.*, vol. 50, pp. 1587-1590, May 16, 1983.

[2] K. Kato, G. Benford, and D. Tzach, "Detailed spectra of high-power broadband microwave emission from interactions of relativistic electron beams with weakly magnetized plasmas," *Phys. Fluids*, vol. 26, pp. 3636-3649, December 1983.

[3] M. S. Di Capua, J. F. Camacho, E. S. Fulkerson, and D. Meeker, "Microwave emission and beam propagation measurements in a high-power relativistic electron beam-plasma system," *IEEE Trans. Plasma Sci.*, vol. 16, pp. 217-224, April 1988.

[4] J. F. Camacho, M. S. Di Capua, E. S. Fulkerson, J. Johnston, and D. Meeker, "Real-time density measurements of a beam-plasma interaction," *Bull. Am. Phys. Soc.*, vol. 32, p. 1868, October 1987.

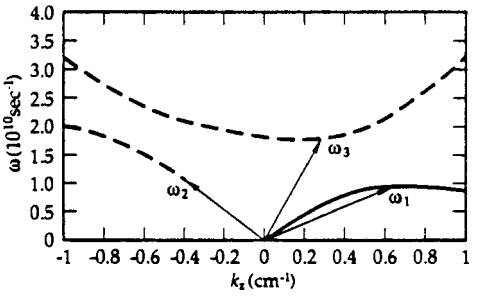

Figure 10—Three-wave mixing process for the ω_p conversion of the emission frequency. The process is $\omega_3 = \omega_1 + \omega_2$ and $k_3 = k_1 + k_2$. Higher order mixing ($\omega_4 = \omega_1 + \omega_3$ and $k_4 = k_1 + k_3$) occurs with higher power.

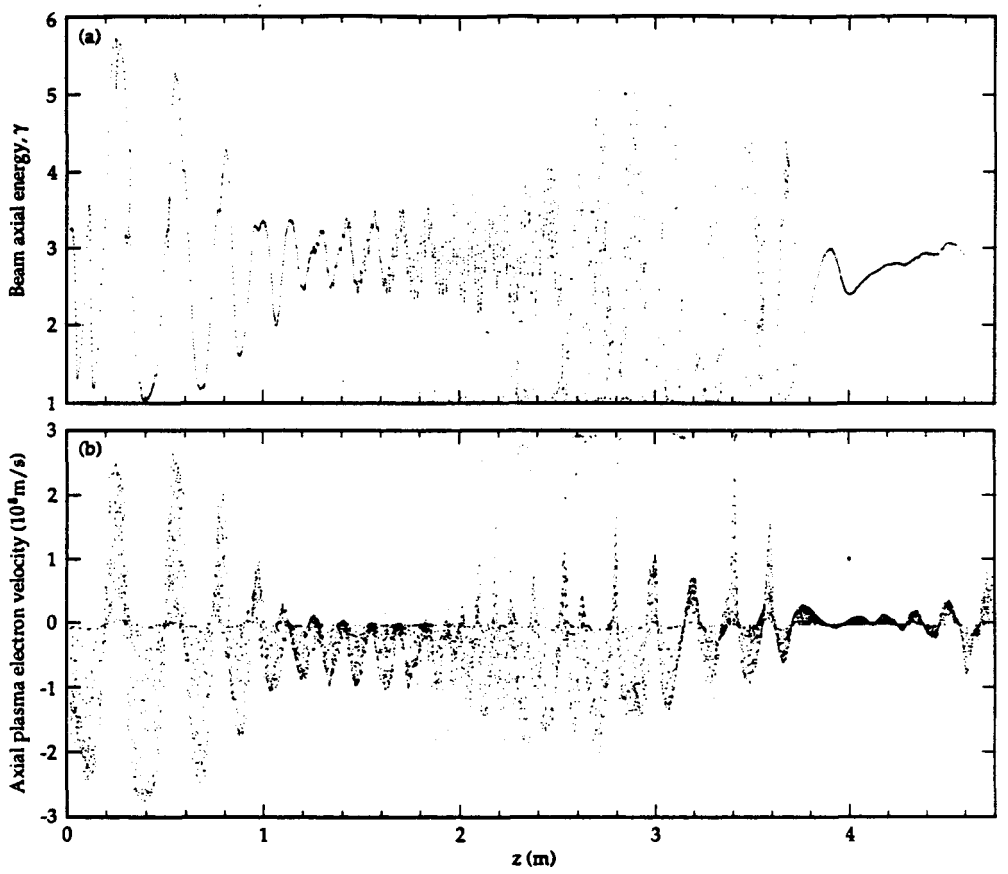

Figure 11—CONDOR simulation of beam behavior in the presence of a very large magnetic field. (a) Beam energy (γ) showing large scale, coherent fluctuations giving rise to electromagnetic radiation. (b) Axial plasma electron phase space showing development of large amplitude oscillations.

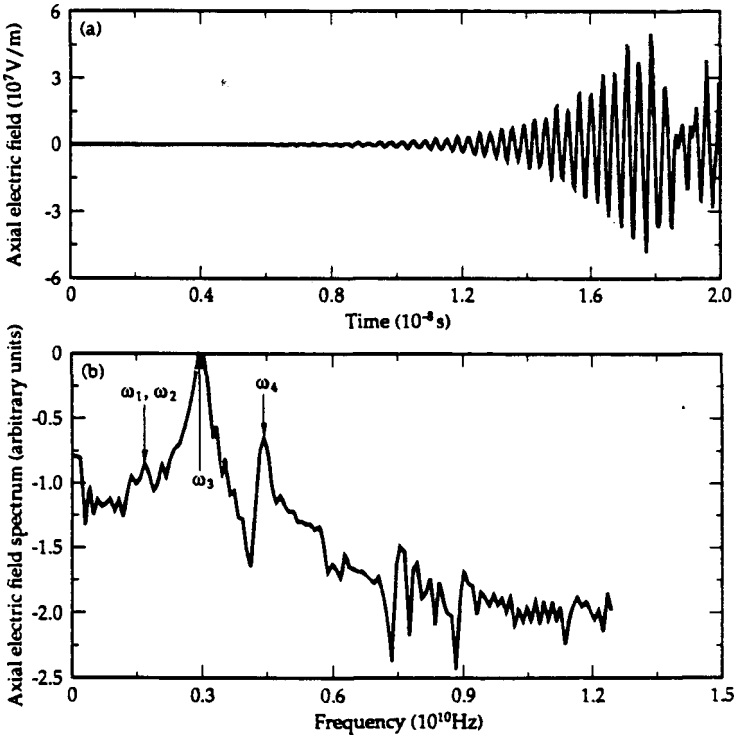

Figure 12—(a) Electric field time history showing development of the instability. (b) Fourier spectrum of the electric field time history showing the frequencies present during wave mixing (compare Fig. 10).